Formation of the Lunar Highlands Mg-suite as told by Spinel

Revision 1

Tabb C. Prissel, Stephen W. Parman, and Jim W. Head

Department of Earth, Environmental, & Planetary Sciences
Brown University, Providence, Rhode Island 02912

Abstract

Two competing hypotheses suggest lunar Mg-suite parental melts formed **(1)** by shallow-level partial melting of a hybridized source region (containing ultramafic cumulates, plagioclase-bearing rocks and KREEP), producing a plagioclase-saturated, MgO-rich melt or **(2)** when plagioclase-undersaturated, MgO-rich melts were brought to plagioclase saturation during magma-wallrock interactions within the anorthositic crust. To further constrain the existing models, phase equilibria experiments have been performed on a range of Mg-suite parental melt compositions to investigate which composition can best reproduce two distinct spinel populations found within the Mg-suite troctolites – chromite-bearing ($FeCr_2O_4$) troctolites and the more rare pink spinel ($MgAl_2O_4$, or Mg-spinel) troctolites (PST).

Phase equilibria experiments at 1-atm pressure were conducted under reducing conditions (log fO_2 ~IW – 1) and magmatic temperatures (1225 – 1400^{o}C) to explore the spinel compositions produced from melts predicted by the models above. Additionally, the experimental data are used to calculate a Sp-Ol, Fe-Mg equilibrium exchange coefficient to correct natural spinel for sub-solidus re-equilibration with olivine in planetary samples: Sp-Ol $K_D^{Fe\text{-}Mg} = 0.044Cr\#_{sp} + 1.5$ ($R^2 = 0.956$). Melts from each model (≥ 50% normative anorthite) produce olivine, plagioclase and Mg-spinel compositionally consistent with PST samples. However, chromite was not produced in any of the experiments testing current Mg-suite parental melt compositions. The lack of chromite in the experiments indicates that current estimates of Mg-suite parental melts can produce Mg-spinel bearing PST, but not chromite-bearing troctolites and dunites. Instead, model calculations using the MAGPOX equilibrium crystallization program predict chromite production from plagioclase-undersaturated melts (< 20% normative anorthite). If so, experimental and model results suggest chromite in Mg-suite crystallized from plagioclase-

undersaturated parental melts, whereas Mg-spinel in the PST is an indicator of magma-wallrock interactions within the lunar crust (a mechanism that increases the normative anorthite contents of initially plagioclase-undersaturated melts, eventually producing Mg-spinel). The constraints for magmatic chromite crystallization suggest Mg-suite parental melts were initially plagioclase-undersaturated. In turn, a plagioclase-undersaturated Mg-suite parent is consistent with mantle overturn models that predict Mg-suite parent magmas resulted from decompression melting of early ultramafic cumulates produced during the differentiation of a global lunar magma ocean.

Introduction

The lunar highlands Mg-suite samples are comprised of plutonic to hypabyssal igneous rock fragments and clasts including dunites, troctolites, pink spinel troctolites, norites, and gabbronorites [e.g. *James* 1980; *Warren* 1993; *Papike et al.,* 1998; *Shearer et al.,* 2015]. Primitive olivine, orthopyroxene (high-Mg# = Fo# = Mg/[Mg + Fe]x100), and calcic-plagioclase (high-An# = Ca/[Ca + Na + K]x100) dominate the mineralogy of Mg-suite samples. Mg-suite rocks are also among the most ancient samples returned from the Moon, dating to > 4.1 Ga [e.g. *Nyquist and Shih* 1992, *Borg et al.,* 2013; *Carlson et al.,* 2014]. The primitive mineralogy combined with ancient ages indicate Mg-suite samples can provide insight into the early lunar interior and magmatic activity post-dating the differentiation of a global magma ocean [*Wood et al.,* 1970, *Smith et al.,* 1970, *Walker et al.,* 1975, *Drake* 1976, *Norman & Ryder* 1979; *James* 1980; *Nyquist & Shih* 1992; *Warren* 1993; *Shearer et al.,* 2006; *Elardo et al.,* 2011; *Borg et al.,* 2013, 2015; *Carlson et al.,* 2014; *Shearer et al.,* 2015].

A positive correlation between the Mg# of mafic minerals and the An# of plagioclase suggests that Mg-suite rock types are comagmatic (i.e., related by a common parental magma crystallizing at < 0.3 GPa) [e.g. *Walker et al.,* 1976; *James* 1980; *Warren* 1986, *Shearer and Papike* 2005; *Carlson et al.,* 2014]. Consistent with a common source, Mg-suite whole rock analyses fall along a Lu-Hf isochron [*Carlson et al.,* 2014]. However, Mg-suite samples also contain an evolved trace element signature (KREEP – K, rare earth element, and P) [e.g. *Warren* 1986; *Hess* 1994; *Papike et al.,* 1998; *Shervais and McGee* 1998; *Shearer and Papike* 2005; *Longhi et al.,* 2010; *Elardo et al.,* 2011]. The pairing of primitive major element chemistry with an evolved trace element signature indicates a more complex origin than crystal fractionation alone [e.g. *Hess* 1994; *Longhi et al.,* 2010; *Elardo et al.,* 2011; *Shearer et al.,* 2015].

Along with elevated trace element concentrations, the pairing of forsteritic olivine and anorthitic plagioclase in the Mg-suite troctolites also suggests an unusual petrogenesis [e.g. *Warren* 1986; *Hess* 1994; *Wieczorek et al.,* 2006; *Longhi et al.,* 2010; *Shearer et al.,* 2015]. First, the high-Fo# olivines constrain Mg-suite parental melts to have Mg#'s ≥ 86, which would be the most primitive melt composition on the Moon and suggests the Mg-suite parent is the least fractionated melt of the lunar mantle [e.g. *Warren* 1986; *Hess* 1994; *Longhi et al.,* 2010]. Second, the pairing of forsteritic olivine with anorthitic plagioclase is unexpected since most basaltic melts fractionate olivine (reducing the Mg# of the melts) prior to plagioclase saturation [e.g. *Green et al.,* 1971, *Hess* 1994]. In this scenario, plagioclase precipitates with relatively FeO-rich olivine (inconsistent with observed troctolite mineralogy).

Two competing petrogenetic models can explain the pairing of anorthitic plagioclase and forsteritic olivine as well as the observed trace element enrichment within Mg-suite troctolites: **(1)** shallow-level partial melting of a hybridized source region (containing ultramafic cumulates, plagioclase-bearing rocks and KREEP) produces plagioclase-saturated, MgO-rich melts with a KREEP signature [*Hess* 1994; *Shearer and Papike,* 1999, 2005; *Longhi et al.,* 2010; *Elardo et* *al.,* 2011] and **(2)** plagioclase-undersaturated, MgO-rich melts are brought to plagioclase saturation during magma-wallrock interactions with the lunar anorthositic crust (and KREEP) [e.g. *Warren and Wasson* 1980; *Longhi* 1981; *James and Flohr* 1983; *Warren* 1986; *Ryder* 1991; *Shervais and McGee* 1998, *Morgan et al.,* 2006; *Prissel et al.,* 2014a]. Both models invoke the production of MgO-rich melts via cumulate mantle overturn [*Hess and Parmentier*, 1995; *Zhong et al.,* 2000; *Elkins Tanton et al.,* 2002; *Laneuville et al.,* 2013]. See *Shearer et al.,* [2015] for a recent summary of Mg-suite petrogenetic models.

Models **(1)** and **(2)** primarily focus on the major mineralogy (olivine and plagioclase) and/or the enriched trace element concentration of the Mg-suite samples. Similarly, existing experimental studies focus on the composition of the major minerals and phases involved in assimilation and/or plagioclase dissolution on the Moon [e.g., *Walker* 1973; *Grove and Bence* 1979; *Warren* 1986; *Finilla* 1994; Hess 1994; *Morgan et al.,* 2006; *Longhi et al.,* 2010; *Elardo et al.,* 2011]. The present study explores the composition of the accessory mineral spinel within the Mg-suite to further constrain existing petrogenetic models.

Premise

Spinel is commonly observed in the lunar troctolites as anhedral to euhedral mineral grains and also inclusions within both olivine and plagioclase indicating it is a primary crystallization product of the Mg-suite parent magma [e.g. *Prinze et al.,* 1973; *Albee et al.,* 1974; *Dowty et al.,* 1974; *Dymek et al.,* 1975; *Baker and Herzberg* 1980; *Lindstrom et al.,* 1984; *Shervais et al.,* 1984; *Marvin et al.,* 1988; *Snyder et al.,* 1998, 1999]. A few Mg-suite samples also exhibit symplectite assemblages containing Cr-spinel, which may be the result of secondary, subsolidus processes. For example, lunar troctolite 76535 is unique in that it contains both anhedral chromite grains and chromite inclusions within olivine, but also a small portion of vermicular intergrowths (or, “symplectite assemblages”) of Cr-spinel + high-Ca pyroxene +/- low-Ca pyroxene [*Gooley et al.,* 1974; *Dymek et al.,* 1975; *Elardo et al.,* 2012]. Previous studies have concluded the Cr-rich symplectite assemblages of Cr-spinel and two pyroxenes are the result of low-pressure olivine (hosting chromite inclusions) + melt reactions to form pyroxene [*Dymek et al.,* 1975]. More recently however, the symplectites in 76535 have been interpreted to be the result of Fe- and Cr-rich metasomatic liquids [*Elardo et al.,* 2012]. Regardless, the present study focuses on the compositions reported for primary, magmatic spinel grains within the Mg-suite samples to compare to experimentally produced spinel in order to better understand the primary processes involved in the formation of Mg-suite lithologies on the Moon.

The presence and composition of primary, magmatic spinel is widely used in terrestrial basaltic systems to place constraints on formation conditions since spinel is commonly observed as an accessory mineral within olivine-bearing igneous rocks [e.g., *Irvine* 1965, 1967; *Dick and Bullen* 1984; *Allan et al.,* 1988; *Kamenetsky et al.,* 2001]. Spinel also exhibits distinct spectral properties and is an important mineral in remote sensing studies aimed at characterizing the geology of the lunar surface [e.g. *Pieters et al.,* 2010, 2014; *Gross and Treiman* 2011; *Prissel et al.,* 2012, 2014a; *Williams et al.,* 2012, in press; *Sun et al.* 2013; *Yamamoto et al.* 2013; *Vaughan et al.* 2013; *Cheek and Pieters* 2014; *Gross et al.,* 2014; *Isaacson et al.,* 2014; *Jackson et al.,* 2014; *Shearer et al.,* 2015; *Treiman et al.,* 2015]. Within the Mg-suite troctolites and dunites, magmatic spinel is an accessory mineral (1 – 13 vol.%) relative to olivine and plagioclase with the exception of ~30 vol.% in ALHA 81005 [*Gross and Treiman* 2011]. Quantifying true modes within the Mg-suite is problematic because of the small clasts that comprise much of the sample set (350 x 150 μm in the case of ALHA 81005) [e.g. *Warren* 1993; *Papike et al.,* 1998; *Gross* *and Treiman* 2011].

Two distinct magmatic spinel populations exist within the Mg-suite troctolites (Fig. 1). The pink spinel in the eponymous pink spinel troctolites (PST) is magnesium-rich and chromium-poor (nearly end-member $MgAl_2O_4$, or Mg-spinel) [e.g., *Prinz et al.,* 1973; *Marvin et al.,* 1988; *Snyder et al.,* 1998; *Prissel et al.,* 2014b]. Spinel in the second group of troctolites (and dunites) is relatively FeO- and Cr_2O_3-rich, existing as chromian spinel or chromite ($FeCr_2O_4$) [*Albee et al.,* 1974; *Dymek et al.,* 1975; *Lindstrom et al.,* 1984; *Elardo et al.,* 2012; *Shearer et al.,* 2015]. In general, Mg-suite spinel compositions trend from chromite within the troctolites and dunites to Mg-spinel in the PST, indicative of the reciprocal substitutions (Mg-Fe^{2+} and Al-Cr) in normal spinel [*Deer et al.,* 1962; *Irvine* 1965; *Haggerty* 1973].

To investigate the origin of magmatic spinel in the Mg-suite, melt compositions consistent with models **(1)** and **(2)** above were synthesized. Each composition was then used in a series of high-temperature (1225 – 1400^{o}C), 1-atm phase equilibria experiments, which produce a range of spinel compositions. Mg-suite rocks are thought to have formed at depths from the base of the lunar crust (< 0.3GPa) up to a kilometer below the surface [e.g., *McCallum & O'Brien* 1996]. Additionally, Mg-suite troctolites are restricted to the low-pressure environments because olivine and plagioclase are not in equilibrium at pressures exceeding ~ 0.3 GPa, [*Andersen* 1915; *Roeder and Osborn* 1966; *Morse* 1980; *Sen and Presnal* 1984]. Under anhydrous conditions, such low pressures have minimal effect on phase equilibria [e.g., *Walker et al.,* 1976; *Prissel et al.,* 2014a]. Therefore, the results from 1-atm phase equilibria experiments are applicable to Mg-suite crystallization within the low-pressure regime of the lunar crust. Experiments testing melts from each model produce olivine, plagioclase and spinel that are compositionally consistent with PST samples. However no chromite was produced in this study, indicating a different melt composition is required to produce the chromite-bearing Mg-suite troctolites. Model calculations using the MAGPOX equilibrium crystallization program [*Longhi et al.,* 1991; *Davenport et al.,* 2014] predict chromite crystallizes from plagioclase-undersaturated parental melts (i.e., melts with low-normative anorthite contents). Experimental and model data therefore indicate a range of melt compositions are required to explain the production of both chromite and Mg-spinel in the Mg-suite troctolites.

Experimental Methods

The parental melt composition derived from model **(1)** [*Longhi et al.,* 2010] is in equilibrium with Fo95 olivine (Mg# ~95) and has a high normative anorthite component (~50% An, Table 1). *Longhi et al.,* [2010] report this melt is capable of producing both forsteritic olivine and calcic-plagioclase consistent with the natural troctolite samples. However, spinel was not considered. Because the Mg-suite parental melt reported by *Longhi et al.,* [2010] can explain the major mineralogy of the Mg-suite troctolites, it was selected as our starting composition A in order to also test the composition of spinel produced.

Depending on the degree of contamination, melt compositions produced in model **(2)** could span a wide range in normative anorthite content, but should still be in equilibrium with Fo95 olivine. On the basis of this criterion, starting compositions B, C, and D were estimated by holding the Mg# of composition A constant while systematically increasing its initial normative anorthite content by ~10, 15, and 25% An, respectively (Table 1). Each calculated starting composition was synthesized using reagent grade oxides and conditioned at IW within a horizontal gas-mixing (H_2 + CO_2 continuous flow) furnace at 900°C for 24 hours. Conditioned powders were pressed (dry) into pellets and affixed to 0.10 mm diameter Re-wire loops. Re-wire was selected as an alternative to Pt-wire because of the minimal (< 15%) FeO-loss expected at the experimental conditions explored here (see *Borisov and Jones* [1999] for a detailed evaluation of Re-wire in 1-atm loop experiments). Experimental charges were then glassed at 1400°C within a Deltech 1-atm vertical gas-mixing furnace (CO-CO_2 continuous flow) at ~ IW – 1 for three hours before drop-quenching into water.

The phase equilibria experiments follow the same methods described above. Experimental runs are held at temperature for 24 hours and then drop-quenched into water. After the drop quench, experimental charges were mounted in epoxy and prepped for electron microprobe analyses. Experimental conditions and results of all experiments are given in Table 2.

All experimental crystalline phases were analyzed using a CAMECA SX 100 Electron Microprobe (Brown University), with a focused beam, accelerating voltage of 15 kV, and beam current of 20 nA. Glass was measured using a diffuse beam (~20 µm). Elements were set to 45s count times with the exception of Na (30s). Na concentrations were calculated by extrapolating time-resolved Na counts to time = 0 (sub-counting for three sets of 10 seconds). Microprobe analyses for each glassed starting composition are reported in Table 1 and all phase compositions are reported in Appendix Table 2.

Results

Results from phase equilibria experiments performed in this study at 1-atm and controlled lunar-like fO_2 (~ IW – 1) produced assemblages of liquid (Liq), Liq + olivine (Ol), Liq + Ol + spinel (Sp), Liq + Sp, Liq + Sp + plagioclase (Pl) and finally (Liq + Ol + Pl). Low sums of the residuals squared were calculated during mass balancing of run products (Table 2). Re-metal was not detected in any of the glass analyses. A few experiments contained small (< 5µm) Re-metal crystals suspended in the glass phase. Minimal FeO-loss (~11% throughout) to the Re-wire occurred in the experiments during 24hr duration as expected [*Borisov and Jones* 1999]. However, each melt investigated produced olivine compositionally consistent with the natural Mg-suite samples (moreover, all Mg-suite parental melt compositions are theoretical and the total FeO content of parental melts are not well constrained). Thus, the similarity between experimental olivine produced in this study and olivine observed in the Mg-suite samples suggests phase equilibria data reported herein is directly applicable to models of Mg-suite petrogenesis. A summary of the experimental conditions, phases present, and calculated modal abundances is provided in Table 2. Averaged phase compositional data for each run is reported in Appendix Table 2.

Testing for Equilibrium

Phases in each run appear chemically homogeneous with euhedral to subhedral mineral grains (Fig. 2). The mineral-melt partition coefficient, K_D (Fe^{2+}–Mg cation fraction exchange coefficient; defined by the $[X_{Fe}/X_{Mg}]^{min} \times [X_{Mg}/X_{Fe}]^{melt}$), for olivine-melt is 0.30 +/- 0.01. The K_D reported here is consistent with other independent studies [e.g. *Elkins-Tanton et al.,* 2003; *Wan et al.,* 2008] performed at similar conditions, but with various starting compositions.

Liquid Lines of Descent

All relevant phase boundary experiments are shown in forsterite-anorthite-quartz pseudo ternary space (Fig. 3).

The liquid line of descent (LLD) for composition A is as follows: Liq → Liq + Ol → Liq + Ol + Sp → Liq + Ol + Sp + Pl → Liq + Ol + Pl. Olivine is the primary liquidus phase, precipitating between 1350 – 1400°C. Olivine continues to precipitate until reaching the Ol + Sp divariant between 1300 – 1280°C. Experimental temperatures investigated in this study did not produce the peritectic assemblage (Liq + Ol + Sp + Pl). However, the loss of spinel at T < 1280°C indicates melt A went through a ternary peritectic resorption reaction (Liq + Ol + Sp → Liq + Ol + Pl) between 1225 – 1280°C. Melt A also reaches the Ol + Pl cotectic between 1225 – 1280°C.

The LLD for composition D follows the order: Liq → Liq + Pl → Liq + Pl + Sp → Liq + Pl + Sp + Ol → Liq + Pl + Ol. The assemblage Liq + Pl was not produced at the temperatures considered. However, plagioclase is estimated to be the original liquidus phase as indicated by the modal abundance accumulated by 1350°C relative to the amount of spinel present (Table 2). Thus, composition D has plagioclase on the liquidus at temperatures between 1350 – 1400°C and also reaches the Pl + Sp divariant within the same temperature range. Melt D follows the Pl + Sp divariant until reaching the ternary peritectic point between 1280 – 1300°C indicated by the presence of spinel at 1300°C and loss of spinel (appearance of olivine) at 1280°C. Thus, Melt D has reached the Pl + Ol cotectic between 1280 – 1300°C and continues co-precipitating the two phases between 1225 - 1280°C.

The LLD for compositions B and C are similar and therefore discussed concurrently. Both compositions B and C produced higher modal abundances of spinel relative to compositions A and D (Table 2). In fact, composition B failed to reach the Sp + Pl divariant at 1300°C, producing only Liq + Sp. Composition C likely began precipitating Liq + Sp, but quickly reached the Liq + Sp + Pl divariant as indicated by the presence of plagioclase at 1300°C.

This is a preprint, the final version is subject to change, of the American Mineralogist (MSA)
Cite as Authors (Year) Title. American Mineralogist, in press.
(DOI will not work until issue is live.) DOI: http://dx.doi.org/10.2138/am-2016-5581

Mineral Chemistry

Spinel

Mg-spinel (~1 – 10μm in diameter throughout) is mostly euhedral and displays an octahedral form with high optical relief relative to the glass (Fig. 2). Spinel grains were too small to obtain reliable compositional profiles to test for zoning, as some spinel exhibit bright rims in BSE imaging. However, each polished grain surface represents a unique dissection distance from the spinel nuclei. Thus, the low standard deviations from EMP analyses suggest chemical zoning, if any, was minimal.

Stoichiometry indicates A-site occupancy (Mg + Fe^{2+} + Mn in normal spinel) is 1.01 +/- .01 cations/4O (2σ standard deviations reported herein) assuming all measured iron is FeO, reflecting a low (~IW – 1) oxygen fugacity. Spinel compositions are near end-member Mg-spinel. Spinels produced by melt A (initial %An ~50) exhibit the greatest variability in composition (Run A6: Cr# = 13 +/- 3, Mg# = 90.6 +/- 0.6; Run A7: Cr# = 13 +/- 2, Mg# = 90.4 +/- 0.5). Compositions B and C (%An ~60, 65 respectively) produce spinel compositions within 2σ of each other (Run B1: Cr# = 6 +/- 1, Mg# = 93.4 +/- 0.3; Run C1: Cr# = 6.2 +/- 0.9, Mg# = 93.6 +/- 0.2). Spinel produced from composition D (%An ~75) are less FeO- and Cr_2O_3-rich than spinel produced in B and C (Run D2: Cr# = 4.3 +/- 0.2, Mg# = 94.4 +/- 0.2; Run D3: Cr# = 5.0 +/- 0.9, Mg# = 93.8 +/- 0.2). Partition coefficients for Mg, Al, and Fe in spinel range from D_{Mg} ~ 5 – 6, D_{Al} ~ 8 – 9, and D_{Fe} ~ 1 – 2 throughout the experimental series. The partitioning of Cr is more variable ranging from D_{Cr} ~ 59 – 81 in melts B, C, and D and D_{Cr} ~ 117 – 129 in melt A.

Olivine

Olivine is consistently forsteritic in composition ranging from Mg# ~92 – 95. Euhedral to subhedral olivine grains were observed throughout the entire A-series and also in runs D5 and D4. Compositions B and C did not produce olivine. Grain size is typically 10-50μm in diameter throughout (Fig. 2). Olivine stoichiometry of M1-site occupancy (Mg + Fe + Mn + Ca) shows excellent totals of 2.00 +/- 0.01 cations/4O. Olivine in composition A evolved from Fo# = 95.7 +/- 0.1 (1330^{o}C) to Fo# = 92.4 +/- 0.5 at lower temperatures (1225^{o}C). Olivine did not precipitate from composition D until 1280^{o}C (D5: Fo# = 94.4 +/- 0.2), resulting in a higher Mg/Fe in the melt and thus, higher Mg/Fe olivine relative to A at the same temperature (D4: Mg# = 93.7 +/- 0.3 at 1225^{o}C). The mineral-melt Cr partition coefficient (D_{Cr}) is ~2 throughout. Al-conentrations in olivine are below detectable limits in all but two runs, which have D_{Al} ~ 0.01.

Plagioclase

Euhedral lathes of plagioclase were observed throughout D-series experiments ranging from 5 - 25μm in width and up to ~60μm in length (Fig. 2). Because of the initially low Na_2O and K_2O contents in each starting composition, plagioclase compositions are both uniformly and highly anorthitic (An# = [Ca/(Ca + Na + K)] x 100 > 97) spanning the entire compositional and temperature range investigated.

Discussion

Melt compositions predicted by both the hybridized source region and assimilation models do not yield chromite and produce Mg-spinel only. Thus, the high normative anorthite melts explored here are capable of producing spinel consistent with the pink spinel troctolites (PST),

This is a preprint, the final version is subject to change, of the American Mineralogist (MSA)
Cite as Authors (Year) Title. American Mineralogist, in press.
(DOI will not work until issue is live.) DOI: http://dx.doi.org/10.2138/am-2016-5581

but not the chromite-bearing troctolites (and dunites). Is either model capable of producing chromite? In the following sections, natural spinels are corrected for sub-solidus re-equilibration using experimental data. Corrected natural spinel compositions are then compared to both experimental and model data in order to determine the parental melt compositions necessary to explain the range of chromite to Mg-spinel in the Mg-suite troctolites. Finally, implications stemming from the spinel constraints are discussed in context with current Mg-suite petrogenetic models.

Correcting for Sub-Solidus Re-Equilibration

The Mg# of both olivine and spinel can be affected by sub-solidus re-equilibration regardless of origin [*Irvine,* 1965, 1967; *Roeder et al.,* 1979; *Jamieson and Roeder,* 1984; *McCallum and Schwartz* 2001]. Evidence for sub-solidus processes exists within the lunar troctolites in the form of symplectite assemblages (that may have formed via metasomatism) [e.g., *Dymek et al.,* 1975; *Elardo et al.,* 2012] and also the rare occurrence of cordierite (e.g., PST 15295 *Marvin et al.,* 1988]. The pairing of cordierite-forsterite-spinel is not in equilibrium at pressures exceeding 0.25 GPa [*Marvin et al.,* 1988]. *Marvin et al.,* [1988] conclude high-T, low-P metamorphic recrystallization of corundum-normative, spinel troctolite lithologies occurred within the lunar crust to form cordierite in situ. Our experimental results support the conclusions of *Marvin et al.,* 1988, as no cordierite precipitated during equilibrium crystallization from any of the starting compositions explored. Because of the evidence for sub-solidus processes, natural data must be corrected for sub-solidus re-equilibration prior to comparison with phase-equilibria experiments. Below, we demonstrate how the experimental results can be used to both identify and correct for sub-solidus re-equilibration between olivine and spinel in planetary samples.

Using phase equilibria data from this study in conjunction with data of *Wan et al.,* [2008], we calculate a Sp-Ol, Fe-Mg equilibrium exchange coefficient (Sp-Ol $K_D^{Fe\text{-}Mg} = [X_{Fe}/X_{Mg}]^{Sp} \times [X_{Mg}/X_{Fe}]^{Ol}$). Because of the efficiency with which reciprocal substitutions in normal spinel take place at magmatic temperatures, the Sp-Ol K_D is linearly correlated with the Cr# of spinel over a wide range of melt compositions (Fig. 4a),

$$\text{Sp-Ol } K_D^{Fe\text{-}Mg} = 0.044\text{Cr\#}_{sp} + 1.5 \qquad \textbf{(1)}$$

($R^2 = 0.956$ with 2σ error of +/- 0.003 and 0.2 for the slope and intercept, respectively). If sub-solidus re-equilibration has occurred, the apparent Sp-Ol $K_D^{Fe\text{-}Mg}$ of natural data will be greater than equilibrium since spinel incorporates Fe^{2+} from olivine, and so will plot above the equilibrium line in Figure 4a.

The effects of sub-solidus re-equilibration are greatest for the least abundant mineral [*Irvine,* 1965; *McCallum and Schwartz* 2001]. Considering the relative abundances of olivine and spinel in lunar rocks, the modal fraction of olivine to spinel is almost always > 1 [*Prissel et al.,* 2014a] with the exception of ALHA 81005 as noted in the introduction. Because spinel is typically an accessory phase of most igneous rocks, the effects of re-equilibration on olivine are assumed to be negligible (Fig. 4b). Thus, only the Fe/Mg of natural spinel is corrected to the equilibrium line defined in equation **(1)** for comparison with the experimental data (Fig. 4c). For a given Cr# of spinel, the Sp-Ol $K_D^{Fe\text{-}Mg}$ of the lunar dunites and troctolites is consistently greater than equilibrium, indicating sub-solidus re-equilibration has occurred (Fig. 4a). PST samples lie along the equilibrium line, and appear to have experienced minimal sub-solidus re-equilibration.

Comparison of Experimental and Natural Data with Model Results

Experiments testing melt compositions predicted by the hybridized source region and assimilation models produce highly forsteritic-olivine and anorthitic-plagioclase (Fo92 – 96; An# > 97). On average, olivine and spinel observed in PST samples are more MgO-rich than olivine in the troctolites and dunites. Results are therefore most consistent with the highest Fo# olivine in the natural PST samples (Fig. 4b).

Melts predicted by both the hybridized source region and assimilation models produce Mg-spinel only (spinel Cr# 4 - 13, Mg# 90 – 94), consistent with Mg-spinel in the PST samples (Fig. 4c). Thus, both models are capable of explaining the production of PST. However, no chromite was experimentally produced in this study. The lack of chromite in the experiments suggests melts saturated (or nearly saturated) with plaigoclase cannot be parental to the chromite-bearing troctolites (and dunites). Additional melt compositions appear necessary to explain chromite-bearing troctolite lithologies.

Estimating Mg-suite Parental Melt Compositions

Unlike olivine and plagioclase (which can both chemically evolve throughout most of crystallization), the peritectic reaction limits the overall chemical evolution and total modal production of spinel for a given melt. Hence, a single melt cannot reproduce the total compositional range of natural PST spinel (or when considering the four experimental starting compositions collectively, Fig. 4c). Moreover, the problem of producing a wide range of spinel compositions from a single melt is much more severe when considering the range of chromite to Mg-spinel in the Mg-suite as a whole.

The Cr# of spinel is negatively correlated with the normative anorthite content (i.e., total Al_2O_3-content) of a melt [*Kamenetsky et al.,* 2001]. Chromian spinel and chromite are thus, not expected in parental melts initially saturated (or nearly saturated) with plagioclase (melts with Al_2O_3 > 16 wt.%). Instead, melts undersaturated with plagioclase are necessary for chromian spinel and chromite production (even at Cr_2O_3 contents < 0.6 wt.%, *Wan et al.,* 2008).

The equilibrium crystallization program MAGPOX [*Longhi et al.,* 1991; *Davenport* 2014] is used to predict the Cr# of spinel produced from plagioclase-undersaturated Mg-suite parental melts. MAGPOX is well calibrated for lunar compositions and redox states [*Slater et al.,* 2003; *Thompson et al.,* 2003] and is chosen here for its ability to reproduce data similar to the experimental results of composition A (Fig. 3, Table 3), including crystallization sequence, phase compositions, and liquidus temperature (compared to MELTS [*Ghiorso and Sack* 1995; *Asimow and Ghiorso* 1998], which predicts spinel as the primary crystallization phase at temperatures > 1500°C using the same starting composition).

Major element chemistry of plagioclase-undersaturated, Mg-suite parental melts are estimated by removing a typical ferroan anorthosite component (FAN 65315, *Hess* [1989]) from starting composition A, producing melts with normative anorthite contents of 40, 30, 20, and 15% An and approximately the same initial melt Mg# (Table 3). Olivine and spinel compositions are recorded at near-liquidus temperatures and also at plagioclase (or orthopyroxene) saturation, producing a range of possible spinel and olivine compositions for a given melt. Model input compositions and results are reported in Table 3.

Model results are consistent with terrestrial observations, in which the Cr# of spinel is negatively correlated with the %An of the melt (Fig. 4c). Melts with > 20% An do not yield chromite, whereas melts with < 20% An produce chromian spinel and chromite consistent with the troctolites and dunites. Note, melts with < 20% An yield both spinel and olivine compositions similar to the trocotlites and dunites after ~50% crystallization (Table 3, Fig. 4b,c).

Results indicate the chromite-bearing troctolites were produced during the crystallization of plagioclase-undersaturated parental melts (Table 3).

An important distinction is that melts must be saturated (or nearly saturated) with plagioclase *prior to* crystallization in order for Mg-spinel to precipitate. For instance, melts with < 50% An can evolve to plagioclase saturation during crystallization, but do not yield Mg-spinel consistent with the natural PST data (Fig. 4c). Moreover, melts with < 20% An (required for chromite production) reach orthopyroxene saturation prior to plagioclase saturation (Fig. 3, Table 3). Given the Mg-suite troctolites contain only a few modal percent of orthopyroxene, if any [e.g., *Shearer et al.,* 2015], a secondary mechanism may be required to enrich the melt in anorthite to not only produce Mg-spinel in the PST, but also delay significant orthopyroxene precipitation in the lunar troctolites (Fig 3).

Implications

Phase equilibria experiments and model results from this study indicate melts saturated (or nearly saturated) in plagioclase cannot explain the presence of chromite in Mg-suite troctolites and dunites. Melts saturated with plagioclase prior to crystallization produce Mg-spinel only, consistent with Mg-suite PST samples. Results therefore indicate melts derived from the hybridized source region model (85.5% dunite, 10% norite, 3% gabbronorite, and 1.5% KREEP, *Longhi et al.,* 2010) can explain PST assemblages, but not the chromite-bearing troctolites. As will be discussed below, revisions to the hybridized source model are suggested to satisfy the spinel constraints.

What appears most robust however, and should be considered in any successful petrogenetic model, is that melt compositions with a range of normative anorthite contents are needed to explain the wide compositional range of spinel observed within the Mg-suite troctolites (Fig. 4b,c). Below, we review magma-wallrock interactions within the lunar ferroan anorthositic crust. Both experimental and model results suggest magma-wallrock interaction is a viable mechanism to increase the normative anorthite content of initially chromite-bearing, plagioclase-undersaturated Mg-suite parental melts. Here, chromite is interpreted to be a primary crystallization phase from Mg-suite parental magmas that are derived from a non-hybridized, ultramafic cumulate (initially uncontaminated, low-normative anorthite melts). As these melts interact with the anorthositic crust, the magma-wallrock interface becomes enriched in Al-content, eventually producing Mg-spinel. In this scenario, Mg-spinel can be used as a marker for magma-wallrock interactions (precipitating from contaminated, high-normative anorthite melts) [*Morgan et al.,* 2006].

Additionally, the interpretation that Mg-suite parental melts were initially plagioclase-undersaturated is consistent with the differentiation of a global magma ocean (that may have accumulated an ultramafic source region from which, Mg-suite parental melts are derived) [e.g., *Wood et al.,* 1970; *Smith et al.,* 1970; *Walker et al.,* 1975; *Drake* 1976; *Norman & Ryder* 1979]. Cumulate mantle overturn could have resulted in the upwelling and decompression melting of the ultramafic source region [e.g. *Hess* 1994; *Hess and Parmentier* 1995; *Zhong et al.,* 2000; *Elkins Tanton et al.,* 2002]. The weight fraction of melt produced during mantle overturn is pressure dependent (weight fraction of melt ~ 0.10/GPa) [*MacKenzie and Bickle,* 1988]. Assuming the ultramafic source accumulated at 600 – 800km depth, ~30 – 40% melting may have occurred during the upwelling of the ultramafic cumulates [*Hess* 1994]. *Hess* [1994] suggests partial melts from the upwelling ultramafic cumulate would resemble Al_2O_3-poor picrites or komatiitic basalts. Mg-suite parental melts predicted here (< 20% An, Table 3) are compositionally similar to both komatiitic basalts and earlier estimates of Mg-suite parent compositions [*Warren* 1986; *Hess* 1994], but with higher Mg# as defined by the model of *Longhi et al.,* [2010]. Thus, results from this study support cumulate mantle overturn as a mechanism to bring chromite-bearing, plagioclase-undersaturated Mg-suite parental melts toward the surface with subsequent intrusions into, and interactions with, the anothositic crust [e.g. *Hess* 1994; *Hess and Parmentier* 1995; *Zhong et al.,* 2000; *Elkins Tanton et al.,* 2002]. Chromite-bearing, plagioclase-undersaturated Mg-suite parental melts are also dense, perhaps explaining the lack of extrusive Mg-suite samples [*Prissel et al.,* 2013, 2015, accepted]. Early mantle-derived magmas such as the Mg-suite should be hotter (analogous to terrestrial komatiites in the Archean) than younger basalts and would be more capable of assimilating crustal material [e.g. *Nisbet* 1982; *Smith and Erlank* 1982; *Huppert and Sparks* 1985; *Sparks* 1986; *Finilla et al.,* 1994; *Hess* 1994; *Parman et al.,* 1997; *Arndt et al.,* 1998; *Shervais and McGee* 1998; *Grove and Parman* 2004].

Petrogenesis of the Lunar Highlands Mg-suite as told by Spinel

How prevalent were magma-wallrock interactions (the term is used here to encompass generally the processes of contamination, dissolution, assimilation, etc.) within the lunar crust? Several studies have quantified the effects of assimilation and dissolution of plagioclase, concluding magma-wallrock interactions occurred to some degree on the Moon [e.g., *Warren* 1986; *Finilla et al.,* 1994; *Hess* 1994; *Morgan et al.,* 2006] as is observed on Earth [e.g. *DePaolo* 1981; *Huppert and Sparks* 1985, 1988; *Sparks* 1986; *Daines and Kohlstedt,* 1994*; Kelemen et al.,* 1995; *Kelemen and Dick,* 1995*; Morgan and Liang,* 2003]. On Earth, dunite channels (up to 100m wide and several km in length) are formed through preferential dissolution of pyroxene as melts percolate through peridotite and precipitate olivine as the reaction product [*Boudier and*

Nicolas, 1985; *Kelemen et al.,* 2000; *Morgan and Liang,* 2005]. If similar processes occurred within the lunar crust, plagioclase-undersaturated melts could preferentially dissolve plagioclase from anorthosite and precipitate Mg-spinel as the reaction product [*Morgan et al.,* 2006; *Gross and Trieman* 2011; *Prissel et al.,* 2014a].

Difficulties associated with magma-wallrock interactions arise when considering the amount of energy needed to raise the temperature of the lunar crust to its melting point (~ 1200 - 1250^{o}C), and assimilation of a pure anorthosite (solidus temperature of ~ 1450^{o}C) is unlikely [*Warren* 1986; *Finilla et al.,* 1994; *Hess* 1994]. Both the cooling and crystallization of a given magmatic intrusion will release energy, which can work to raise the temperature of the wallrock to its melting point. Previous lunar assimilation models suggest that latent heat released during > 15% crystallization of olivine will decrease the Mg# of the residual Mg-suite parent, precipitating FeO-rich olivine inconsistent with Mg-suite mineralogy [e.g., *Hess* 1994]. However, a range of olivine compositions exists within the Mg-suite, and results from this study indicate > 50% crystallization from plagioclase-undersaturated melts produces olivine compositionally consistent with the range of olivine observed within the lunar troctolites and dunites (Fig. 5).

Moreover, the incorporation of a normative anorthite component in basaltic melts can decrease liquidus temperatures by nearly 200^{o}C (Table 3). This means olivine fractionation may be momentarily delayed in contaminated melts, preserving the high-Mg# of the system. *Morgan et al.,* [2006] verified this effect with plagioclase dissolution experiments, producing both crystal-free and spinel saturated reactive boundary layers near the melt-plagioclase interface. In a similar study, *Prissel et al.,* [2014a] experimentally confirmed the reactive boundary layer between the melt and anorthite is Mg-spinel saturated.

The production of Mg-spinel may be restricted to the melt-rock interface due to the slow diffusion rates for Al_2O_3 in basaltic melts [e.g., *Finilla et al.,* 1994; *Hess* 1994; *Morgan et al.,* 2006]. Thus, if Mg-spinel is produced at a reactive boundary layer during plagioclase dissolution, Mg-spinel-bearing lithologies are expected to represent a volumetrically minor, albeit possibly widespread, component of the lunar crust. Taking the current lunar sample collection at face value then, the paucity of PST and Mg-spinel-bearing samples supports the conclusion that crustal contamination occurred, but was rare and restricted to small volumes of a given intrusion (i.e., the magma-wallrock interface). Although the lunar sample collection may not be entirely representative, remote sensing observations support conclusions that Mg-spinel lithologies are widespread (detections on both the near- and farside of the Moon), but possibly a volumetrically minor constituent of the lunar crust (~20 outcrops globally at the km-scale) [*Pieters et al.,* 2014].

The Apollo 14 high-alumina basalts, which are contemporaneous with the Mg-suite (~4.2 – 4.3 Ga), also contain low Cr# spinel and likely acquired their aluminous chemistry through crustal contamination [e.g. *Steele* 1972; *Taylor et al.,* 1983, *Morgan et al.,* 2006]. The presence of low-Cr spinel in ancient lunar rocks supports models suggesting the thermal state of the early lunar crust was hotter, making assimilation or dissolution more likely [*Andrews-Hanna et al.,* 2013, 2014]. Additionally, a turbulent or replenished dike, sill, or magma reservoir will buffer high-temperatures near the magma-wallrock interface [*Huppert and Sparks* 1988; *Finilla et al.,* 1994; *Morgan et al.,* 2006; *Prissel et al.,* 2014a]. Without a turbulent or replenished magmatic system, the base of the lunar crust would provide the most favorable conditions (higher temperatures relative to the mid-shallow level crust) for magma-wallrock interactions to occur. As the crust ages and cools, assimilation and dissolution of plagioclase should become less prevalent. Little evidence for crustal contamination exists in the younger mare basalts and pristine lunar volcanic glasses [*Finilla et al.,* 1994; *Hess* 1994].

The production of Mg-spinel via magma-wallrock interactions could also explain the lack of sub-solidus re-equilibration in the PST samples relative to the chromite-bearing troctolites (Fig. 4a). If Mg-spinel formed at the magma-wallrock interface within dikes or via reactive porous flow through the anorthositic crust [*Prissel et al.,* 2014a], the effects of sub-solidus re-equilibration should be minor due to rapid cooling rates (e.g., weeks to months for a shallow sill or dike). The disequilibrium between spinel and olivine in the troctolites and dunites (Fig. 4a) indicates slower cooling than PST samples and/or the high olivine/spinel modal fractions expected during equilibrium crystallization from uncontaminated, plagioclase-undersaturated melts (Table 2).

Finally, the distinct spinel-troctolite populations may be the result of a limited lunar sample set. Additional sampling could yield spinel troctolites intermediate in composition to the Mg-spinel-bearing PST and chromite-bearing troctolites (and dunites). However, intermediate Mg-suite spinel compositions will not change the conclusions herein as a spectrum of melt compositions are required to produce the current chromite to Mg-spinel populations.

An Alternative Hybridized Source Region?

It is possible that several source regions, heterogeneous in plagioclase abundance, could produce a variety of melts with respect to normative anorthite content. However, it is physically unclear whether or not several heterogeneous hybridized source regions can be formed, and later re-melted, during mantle overturn. Thus, geophysical modeling on the solid state mixing of early cumulates at the base of the lunar crust is needed to strengthen this hypothesis [*Shearer et al.,* 2015].

An alternative hypothesis could include the hybridization of ultramafic cumulates and KREEP (with little to no plagioclase-bearing cumulates) below or near the base of the lunar anorthositic crust. Melts derived from such a source would contain a KREEP component, bypassing the complications associated with assimilation of KREEP, which could lower the Mg# of the parental melt as originally proposed [*Hess* 1994; *Longhi et al.,* 2010; *Elardo et al.,* 2011]. Based on the constraints presented above, this scenario suggests partial melts from the ultramafic + KREEP hybridized source could fractionate to form chromian spinel and/or interact with the anorthositic crust to produce Mg-spinel.

Note, a KREEP component is required to explain several Mg-suite samples collected during the Apollo and Luna missions. On the other hand, lunar meteorite Dhofar 489, which includes a KREEP-poor Mg-suite-like PST clast [*Takeda et al.,* 2006], and Mg-suite dunite 72415 do not contain a KREEP signature [*Papike et al.,* 1998]. It is possible that the KREEP component measured in several of the returned Mg-suite samples is a factor of nearside sampling near the Procellerum KREEP Terrane [e.g. *Lucey and Cahill* 2009; *Cahill et al.,* 2009; *Taylor* 2009; *Prissel et al.,* 2014a; *Shearer et al.,* 2015].

Implications to Remote Sensing Studies

Remote sensing studies have detected Mg-spinel-dominated (i.e. mafic-poor or mafic free) exposures on the surface of the Moon, termed pink spinel anorthosite or PSA [e.g. *Pieters et al.,* 2010, 2014; *Dhingra et al.,* 2010]. Much debate remains concerning the nature of the lithology, effects of space weathering on composition, and whether or not the lithology is of endogenic or exogenic origins [*Gross and Treiman* 2011; *Prissel et al.,* 2012; *Williams et al.,* 2012; in press; *Vaughan et al.* 2013; *Cheek and Pieters* 2014; *Gross et al.,* 2014; *Isaacson et al.,* 2014; *Jackson et al.,* 2014; *Pieters et al.,* 2014; *Prissel et al.,* 2014a; *Treiman et al.,* 2015]. Mg-spinel is rare among the lunar samples and predominantly associated with the Mg-suite PST, which have been classified as igneous, plutonic and pristine [e.g. *James* 1980; *Warren* 1993; *Papike et al.,* 1998; *Shearer et al.,* 2015]. Results from this study indicate magma-wallrock interactions played a key role in forming Mg-spinel on the Moon. Thus, PSA-type lithologies detected remotely need not invoke exogenic origins. It is more likely the same magma-wallrock interactions involved in producing Mg-spinel within PST (and Apollo 14 high-alumina basalts) also formed the Mg-spinel lithologies detected remotely.

Approximately twenty remote detections of Mg-spinel have been identified globally [*Pieters et al.,* 2014]. The low number of global PSA detections is consistent with conclusions from this study, which suggest Mg-spinel lithologies formed by magma-wallrock interactions and represent a widespread, but volumetrically minor component of the lunar crust. If PSA is used as a proxy for Mg-suite magmatism [*Prissel et al.,* 2014a], results from this study suggest remote detections of Mg-spinel represent areas of turbulent or replenished Mg-suite magmatism (e.g., pulsed injections, stoping, fracturing) that interacted strongly with the crust. If so, the concentration of PSA detections within the nearside southern highlands suggests this is the most promising region to study Mg-suite magmatism [*Pieters et al.,* 2014; *Prissel et al.,* accepted].

Lastly, a key criteria for magma-wallrock interactions on the Moon is the resulting low Cr# spinel expected [*Morgan et al.,* 2006; *Prissel et al.,* 2014a], whereas Cr-rich spinel will precipitate from uncontaminated, low-Al_2O_3 basaltic melts [Kamenetsky et al., 2001; Wan et al., 2008]. Thus, the characterization of spinel Cr-content within the V-NIR can help distinguish between uncontaminated mantle melts and those that have reacted with the crust [*Williams et al.*, 2012; in press]. These are integral factors for remote sensing studies aimed at understanding the distribution and origin of spinel-bearing lithologies on the Moon.

Acknowledgements

The authors would like to thank Paul C. Hess, Malcolm J. Rutherford, Colin R.M. Jackson and Kelsey B. Williams for countless discussions leading to many of the ideas explored in this manuscript. A special thank you to Joseph Boesenberg for assistance with electron-probe analyses, Brad Jolliff for helpful suggestions, and Charles E. Lesher for handling of the manuscript. Two anonymous reviewers helped to strengthen this manuscript and broaden its implications. Research supported by NASA SSERVI contract NNA14AB01A.

References

Allan, J.F., Sack, R.O., Batiza, R., (1988). Cr-rich spinels as petrogenetic indicators; MORB-type lavas from the Lamont seamount chain, eastern Pacific. American Mineralogist. 73 (7–8), 741–753.

Andersen, O. (1915). The System Anorthite-Forsterite-Silica. American Journal of Science. Vol 39. 232. 407 – 454.

Andrews-Hanna, J.C., et al., (2013). Ancient igneous intrusions and early expansion of the Moon revealed by GRAIL. Science 339 (6120), 675–678.

Andrews-Hanna, J.C., et al., (2014). Structure and evolution of the lunar Procellarum region as revealed by GRAIL gravity data. Nature. Vol. 514, p68. DOI:10.1038/nature13697

Arndt, N., et al., (1998). Were komatiites wet? Geology. V. 26. P. 739 – 742.

Asimow, P.D., and Ghiorso, M.S. (1998). Algorithmic Modifications Extending MELTS to Calculate Subsolidus Phase Relations. American Mineralogist. 83, p. 1127 – 1131.

Baker, M.B., Herzberg, C.T., (1980). Spinel cataclasites in 15445 and 72435: petrology and criteria for equilibrium. In: Proceedings of the 11th Lunar & Planetary Science Conference, pp. 535–553.

Bence, A.E., Delano, J.W., and Papike, J.J. (1974). Petrology of the highlands massifs at Taurus-Littrow: An analysis of the 2-4mm soil fraction. Proceedings of the Lunar Science Conference. vol. 5, p. 785.

Borg, L., et al., (2013). Evidence for Widespread Magmatic Activity at 4.36 Ga in the Lunar Highlands from Young Ages Determined on Troctolite 76535. 44th Lunar and Planetary Science Conference, #1563.

Borisov, A. and Jones, J.H. (1999). An evaluation of Re, as an alternative to Pt, for the 1 bar loop technique: An experimental study at 1400^{o}C. American Mineralogist. 84. 1528-1534.

Boudier, F., and Nicolas, A., (1985). Harzburgite and lherzolite subtypes in ophiolitic and oceanic environments. Earth and Planetary Science Letters. 76 (1–2), 84–92.

Cahill, J.T.S., Lucey, P.G., and Wieczorek, M.A. (2009). Compositional variations of the lunar crust: Results from radiative transfer modeling of central peak spectra. Journal of Geophysical Research: Planets, 114(E9), E09001, doi.org/10.1029/2008JE003282.

Carlson, R.W., et al., (2014)._Rb-Sr, Sm-Nd and Lu-Hf isotope systematics of the lunar Mg-suite: the age of the lunar crust and its relation to the time of Moon formation. Philosophical Transactions of the Royal Society A: Mathematical, Physical and Engineering Sciences, vol. 372, issue 2024, pp. 20130246-20130246. DOI: 10.1098/rsta.2013.0246.

Daines, M.J., Kohlstedt, D.L., (1994). The transition from porous to channelized flow due to melt/rock reaction during melt migration. Geophysical Research Letters, 21 (2), 145–148.

Davenport, J.D., et al., (2014). Simulating Planetary Igneous Crystallization Environments (SPICES): A Suite of Igneous Crystallization Programs. 45^{th} Lunar and Planetary Science Conference, #1111.

Deer, W.A., Howie, R.A., and Zussman, J. (1962). Rock Forming Minerals: Non-Silicates Vol. 5. Wiley Publications, NY, NY.

DePaolo, D.J., (1981). Trace element and isotopic effects of combined wallrock assimilation and fractional crystallization. Earth and Planetary Science Letters, 53(2), pp.189–202.

Dhingra, D., et al., (2011). Compositional diversity at Theophilus Crater: understanding the geological context of Mg-spinel bearing central peaks. Geophysical Research Letters, 38 (11).

Dick, H.J.B., and Bullen, T., (1984). Chromian spinel as a petrogenetic indicator in abyssal and alpine-type peridotites and spatially associated lavas. Contributions to Mineralogy and Petrology. 86 (1), 54–76.

Drake, M.J. (1976). Evolution of Major Mineral Compositions and Trace Element Abundances During Fractional Crystallization of a Model Lunar Composition. Geochimica et Cosmochimica Acta. Vol. 40, Issue 4. p. 401-411.

Dymek, R.F., Albee, A.L., and Chodos, A.A. (1975) Comparative petrology of lunar cumulate rocks of possible primary origin: Dunite 72415, troctolite 76535, norite 78235, and anorthosite 62237. Proceedings of the 6th Lunar Science Conference, 301–341.

Elardo, S.M., Draper, D.S., and Shearer, C.K. (2011). Lunar Magma Ocean crystallization revisited: Bulk composition, early cumulate mineralogy, and the source regions of the highlands Mg-suite. Geochimica et Cosmochimica Acta, 75, 3024–3045.

Elardo, S.M., McCubbin, F.M., and Shearer, C.K. (2012). Chromite symplectites in Mg- suite troctolite 76535 as evidence for infiltration metasomatism of a lunar layered intrusion. Geochimica et Cosmochimica Acta, 87, 154–177.

Elkins Tanton, L.T., et al., (2002). Re-examination of the lunar magma ocean cumulate overturn hypothesis: melting or mixing is required. Earth and Planetary Science Letters, 196 (3–4), 239–249.

Elkins-Tanton, L.T., Chatterjee, N., Grove, T.L., (2003). Experimental and petrological constraints on lunar differentiation from the Apollo 15 green picritic glasses. Meteoritics and Planetary Science, 38 (4), 515–527.

Finnila, A.B., Hess, P.C., Rutherford, M.J., (1994). Assimilation by lunar mare basalts: melting of crustal material and dissolution of anorthite. Journal of Geophysical Research, 99 (E7), 14677–14690.

Ghiorso, M.S., and Sack, R.O. (1995). Chemical Mass Transfer in Magmatic Processes IV. A revised and internally consistent thermodynamic model for the interpolation and extrapolation of liquid-solid equilibria in magmatic systems at elevated temperatures and pressures. Contributions to Mineralogy and Petrology, 119, p. 197 – 212.

Gooley, R., et al., (1974). A Lunar rock of deep crustal origin: sample 76535. Geochimica et Cosmochimica Acta. 38, p. 1329 – 1340.

Green, D.H., Ringwood, A.E., Ware, N.G., Hibberson, W.O., Major, A., and Kiss, E. (1971). Experimental petrology and petrogenesis of Apollo 12 basalts. Proceedings of the 2nd Lunar Science Conference, Vol. 1, p. 601 – 615.

Gross, J., Treiman, A.H., (2011). Unique spinel-rich lithology in lunar meteorite ALHA 81005: origin and possible connection to M3 observations of the farside highlands. Journal of Geophysical Research, 116 (E10).

Gross, J., et al., (2014). Spinel-rich Lithologies in the Lunar Highland Crust: Linking Lunar Samples with Crystallization Experiments and Remote Sensing, American Mineralogist, v. 99, p. 1849-1859, doi:10.2138/am-2014-4780.

Grove, T.L., and Bence, A.E. (1979). Crystallization kinetics in a multiply saturated basalt magma: An experimental study of Luna 24 ferrobasalt. Proceedings of the 10th Lunar and Planetary Science Conference. p. 439 – 478.

Grove, T.L., and Parman, S.W., (2004). Thermal evolution of the Earth as recorded by komatiites. Earth and Planetary Science Letters, 219. p. 173 – 187.

Hess, P.C., (1994). Petrogenesis of lunar troctolites. Journal of Geophysical Research, 99 (E9), 19083–19093.

Hess, P.C., Parmentier, E.M., (1995). A model for the thermal and chemical evolution of the Moon's interior: implications for the onset of mare volcanism. Earth and Planetary Science Letters, 134 (3–4), 501–514.

Hiesinger, H., Head, J.W., (2006). New views of lunar geoscience: an introduction and overview. Reviews in Mineralogy and Geochemistry, 60, 1–81.

Hodges, F.N., and Kushiro, I. (1973). Petrology of Apollo 16 lunar highland rocks. Proceedings of the Lunar Science Conference, vol. 4, p.1033.

Huppert, H.E., Sparks, R.S.J. (1985). Cooling and contamination of mafic and ultramafic magmas during ascent through continental crust. Earth and Planetary Science Letters, 74, p. 371 – 386.

Huppert, H.E., Sparks, R.S.J., (1988). The generation of granitic magmas by intrusion of basalt into continental crust. Journal of Petrology, 29 (3), 599–624.

Irvine, T.N., (1965). Chromian spinel as a petrogenetic indicator: Part 1. Theory. Canadian Journal of Earth Science. 2 (6), 648–672.

Irvine, T.N., (1967). Chromian spinel as a petrogenetic indicator: Part 2. Petrologic applications. Canadian Journal of Earth Science. 4 (1), 71–103.

Isaacson, P.J., et al., (2014). Experimental weathering of synthetic spinels. 45th Lunar and Planetary Science Conference, #1612.

Jackson, C.R.M., et al., (2014). Visible-infrared spectral properties of iron-bearing aluminate spinel under lunar-like redox conditions. American Mineralogist, 99, 1821 – 1833. http://dx.doi.org/10.2138/am-2014-4793.

James, O.B. (1980). Rocks of the early lunar crust. Proceedings of the 11th Lunar and Planetary Science Conference, 365–393.

James, O.B., and Flohr, M.K. (1983). Subdivision of the Mg-suite noritic rocks into Mg-gabbronorites and Mg-norites. Journal of Geophysical Research, 88, Suppl. A603–A614.

Jamieson, H.E., Roeder, P.L., (1984). The distribution of Mg and Fe2+ between olivine and spinel at 1300 degrees C. American Mineralogist, 69 (3–4), 283–291.

Jolliff, B.L., et al., (2000). Major lunar crustal terranes: surface expressions and crust-mantle origins. Journal of Geophysical Research, 105 (E2), 4197–4216.

Kamenetsky, V.S., Crawford, A.J., Meffre, S., (2001). Factors controlling chemistry of magmatic spinel: an empirical study of associated olivine, Cr-spinel and melt inclusions from primitive rocks. Journal of Petrology, 42 (4), 655–671.

Keil, K., Prinz, M., Bunch, T.E., (1970). Mineral chemistry of lunar samples. Science, 167 (3918), 597–599.

Kelemen, P.B., Dick, H.J.B., (1995). Focused melt flow and localized deformation in the upper mantle: juxtaposition of replacive dunite and ductile shear zones in the Josephine peridotite, SW Oregon. Journal of Geophysical Research, 100 (B1), 423–438.

Kelemen, P.B., Shimizu, N., Salters, V.J.M., (1995). Extraction of mid-ocean-ridge basalt from the upwelling mantle by focused flow of melt in dunite channels. Nature, 375 (6534), 747–753.

Kelemen, P.B., Braun, M., Hirth, G., (2000). Spatial distribution of melt conduits in the mantle beneath oceanic spreading ridges: observations from the Ingalls and Oman ophiolites. Geochemistry, Geophysics, Geosystems, 1 (7).

Laneuville, M., et al., (2013). Asymmetric thermal evolution of the Moon. Journal of Geophysical Research, 118 (7), 1435–1452.

Lucey, P.G., and Cahill, J.T.S. (2009). The Composition of the Lunar Surface Relative to Lunar Samples. 40th Lunar and Planetary Science Conference, #2424.

Longhi, J., (1977). Pyroxene stability and the composition of the lunar magma ocean. Proceedings of the 9th Lunar and Planetary Science Conference, p. 285 – 306.

Longhi, J., (1981). Preliminary modeling of high-pressure partial melting: Implications for early lunar differentiation. Proceedings of the 12th Lunar and Planetary Science Conference, p. 1001–1018.

Longhi, J., (1991). Comparative liquidus equilibria of hypersthene-normative basalts at low pressure. American Mineralogist, vol. 76. p. 785 – 800.

Longhi, J., Durand, S.R., Walker, D., (2010). The pattern of Ni and Co abundances in lunar olivines. Geochimica et Cosmochimica Acta, 74 (2), 784–798.

MacKenzie, D. and Bickle, M.J. (1988). The volume and composition of melt generated by extension of lithosphere. Journal of Petrology, 29, 625 – 649.

Marvin, U.B., Carey, J.W., Lindstrom, M.M., (1988). Cordierite-spinel troctolite, a new magnesium-rich lithology from the lunar highlands. Science, 243, 925–928.

McCallum, I.S., Schwartz, J.M., (2001). Lunar Mg suite: thermobarometry and petrogenesis of parental magmas. Journal of Geophysical Research, 106 (E11), 27969–27983.

Morgan, Z., Liang, Y., (2003). An experimental and numerical study of the kinetics of harzburgite reactive dissolution with applications to dunite dike formation. Earth and Planetary Science Letters, 214 (1–2), 59–74.

Morgan, Z., Liang, Y., (2005). An experimental study of the kinetics of lherzolite reactive dissolution with applications to melt channel formation. Contributions to Mineralogy and

Petrology, 150 (4), 369–385.

Morgan, Z., Liang, Y., Hess, P., (2006). An experimental study of anorthosite dissolution in lunar picritic magmas: implications for crustal assimilation processes. Geochimica et Cosmochimica Acta, 70 (13), 3477–3491.

Morse, S.A. (1980). Basalts and Phase Diagrams: An Introduction to the Quantitative Use of Phase Diagrams in Igneous Petrology. Springer-Verlag, New York, Inc.

Nisbet, G.M., (1982). The tectonic setting and petrogenesis of komatiites. In: Komatiites. Allen and Unwin, London. P. 501 – 520.

Norman, M.D., and Ryder, G. (1979). A summary of the petrology and geochemistry of pristine highlands rocks. Proceedings of the 10th Lunar and Planetary Science Conference, 531–559.

Nyquist, L.E., and Shih C.-Y. (1992). The isotopic record of lunar volcanism. Geochimica et Cosmochimica Acta, 56, 2213–2234.

Papike, J.J., Ryder, G., and Shearer, C.K. (1998). Lunar samples. Reviews in Mineralogy, 36, 5-1–5-234.

Parman, S.W., et al., (1997). Emplacement conditions of komatiite magmas from the 3.49 Ga Komati Formation, Barberton Greenstone Belt, South Africa. Earth and Planetary Science Letters, 150. p. 303 – 323.

Prinz, M., et al., (1973). Spinel troctolite and anorthosite in Apollo 16 samples. Science. 179, 74–76.

Pieters, C.M., et al., (2011). Mg-spinel lithology: a new rock type on the lunar farside. Journal of Geophysical Research, 116 (E6).

Pieters, C.M., et al., (2014). The distribution of Mg-spinels across the Moon and constraints on crustal origin. American Mineralogis, 99. 1893 – 1910.

Presnall, D.C., et al., (1979). Generation of Mid-ocean Ridge Tholeiites. Journal of Petrology, Vol. 20. 3 – 35.

Prissel, T.C., et al., (2012). Melt–wallrock reactions on the Moon: experimental constraints on the formation of newly discovered Mg-spinel anorthosites. 43rd Lunar and Planetary Science Conference, #2743.

Prissel, T.C., et al., (2013). Mg-suite plutons: Implications for mantle-derived primitive magma source depths on the Moon. 44th Lunar and Planetary Science Conference, #3041.

Prissel, T.C., et al., (2014a). Pink Moon: The petrogenesis of pink spinel anorthosites and implications concerning Mg-suite magmatism. Earth and Planetary Science Letters, 403, 144–156.

Prissel, T.C., et al., (2014b). Petrogenesis of the Lunar Highlands Mg-suite as told by Spinel. 45th Lunar and Planetary Science Conference, #2514

Prissel, T.C., et al., (2015). Buoyancy Driven Magmatic Ascent of Mg-suite Parental Melts. 46th Lunar and Planetary Science Conference, #1158.

Prissel, T.C., et al., (in review). On the Potential for Mg-suite Extrusive Volcanism.

Roeder, P.L. and Osborn, E.F. (1966). Experimental data for the system MgO-FeO-Fe_2O_3-

$CaAl_2Si_2O_8$-SiO_2 and their petrologic implications. American Journal of Science, Vol. 264, 428 – 480.

Roeder, P.L., Campbell, I.H., Jamieson, H.E., (1979). A re-evaluation of the olivine-spinel geothermometer. Contributions to Mineralogy and Petrology, 68 (3), 325–334.

Ryder, G., (1991). Lunar ferroan anorthosites and mare basalt sources: the mixed connection. Geophysical Research Letters, 18 (11), 2065–2068.

Sen, G., and Presnall, D.C. (1984). Liquidus phase relationships on the join anorthite-forsterite-quartz at 10kbar with applications to basalt petrogenesis. Contributions to Mineralogy and Petrology, 85. 404 – 408.

Shearer, C.K. and Papike, J.J. (1999). Magmatic evolution of the Moon. American Mineralogist, 84, 1469–1494.

Shearer, C.K., & Papike, J.J. (2005). Early Crustal Building Processes on the Moon: Models for the Petrogenesis of the Magnesian Suite. Geochimica et Cosmochimica Acta, Vol. 69, 13. p. 3445-3461.

Shearer, C.K., et al., (2006). Magmatic and thermal history of the Moon. Reviews in Mineralogy and Geochemistry, 60, 365–518.

Shearer, C.K., et al., (2015). Origin of the lunar highlands Mg-suite: An integrated petrology, geochemistry, chronology, and remote sensing perspective. American Mineralogist, 100, pp. 294 – 325. DOI: http://dx.doi.org/10.2138/am-2015-4817

Shervais, J.W., Taylor, L.A., Laul, J.C., and Smith, M.R. (1984). Pristine highland clasts in consortium breccia 14305: Petrology and geochemistry. Journal of Geophysical Research, 89, Suppl. 1, C25–C40.

Shervais, J.W., and McGee, (1998). Ion and electron microprobe study of troctolites, norite, and anorthosites from Apollo 14: Evidence for urKREEP assimilation during petrogenesis of Apollo 14 Mg-suite rocks. Geochimica et Cosmochimica Acta, 62. p. 3009 – 3023.

Slater, V.P., et al., (2003). An Evaluation of the Igneous Crystallization Programs – MELTS, MAGPOX, and COMAGMAT Part II: Impliacations of magmatic fO_2. 34^{th} Lunar and Planetary Science Conference, #1896.

Smith, J.V., et al., (1970). Petrologic History of the Moon Inferred from Petrography, Mineralogy and Petrogenesis of Apollo 11 Rocks. Proceedings of the Apollo 11 Lunar Science Conference, Vol. 1. p. 897-925.

Smith, H.S., and Erlank, A.J., (1982). Geochemistry and petrogenesis of komatiites from the Barberton Greenstone belt, South Africa. In: Komatiites. Allen and Unwin, London. P. 347 – 398.

Snyder, G.A., et al., (1998). Journey to the center of the regolith: a spinel troctolite and other clasts from drive tube 68001. 29^{th} Lunar and Planetary Science Conference, #1144.

Snyder, G.A., et al., (1999). Mineralogy and petrology of a primitive spinel troctolite and gabbros from Luna 20, eastern highlands of the Moon. 30^{th} Lunar and Planetary Science Conference, #1491.

Sparks, R.S.J. (1986). The role of crustal contamination in magma evolution through geological time. Earth and Planetary Science Letters, 78, p. 211 – 223.

Steele, I.M., (1972). Chromian spinels from Apollo 14 rocks. Earth and Planetary Science Letters, 14 (2), 190–194.

Sun, Y., Li, L. & Zhang, Y.Z., (2013). Detection of Mg-Spinel Bearing Central Peaks Using M3 Images. 44th Lunar and Planetary Science Conference, #1393.

Takeda, H., et al., (2006). Magnesian anorthosites and a deep crustal rock from the farside crust of the moon. Earth and Planetary Science Letters, 247, 171–184.

Taylor, LA., et al., (1983). Pre-4.2 AE mare-basalt volcanism in the lunar highlands. Earth and Planetary Science Letters, 66, p. 33 – 47.

Taylor, G.J. (2009). Ancient Lunar Crust: Origin, Composition, and Implications. Elements, Vol 5. p. 17 – 22.

Thompson, C.K., et al., (2003). An Evaluation of the Igneous Crystallization Programs – MELTS, MAGPOX, and COMAGMAT Part 1: Does One Size Fit All? 34th Lunar and Planetary Science Conference, # 1881.

Treiman, A.H., Gross, J., and Glazner, A.F. (2015). Lunar Rocks rich in Mg-Al spinel: Enthalpy constraints suggest origins by impact melting. 46th Lunar and Planetary Science Conference, #2518.

Vaughan, W.M., et al., (2013). Geology and petrology of enormous volumes of impact melt on the Moon: a case study of the Orientale basin impact melt sea. Icarus, 223 (2), 749–765.

Walker, D., et al., (1973). Origin of Lunar Feldspathic Rocks. Earth and Planetary Science Letters, 20, 325 – 336.

Walker, D., Longhi, J., & Hays, J.F. (1975). Differentiation of a Very Thick Magma Body and Implications for the Source Regions of Mare Basalts. Proceedings of the 6th Lunar Science Conference, p. 1103-1120.

Walker, D., et al., (1976). Crystallization history of lunar picritic basalt sample 12002 – phase-equilibria and cooling-rate studies. Geological Society of America Bulletin, 87, 646–656.

Wan, Z., Coogan, L.A., and Canil, D. (2008). Experimental calibration of aluminum partitioning between olivine and spinel as a geothermometer. American Mineralogist, 93. 1142 – 1147.

Warren, P.H. and Wasson, J.T. (1980). Further foraging for pristine nonmare rocks: Correlations between geochemistry and longitude. Proceedings of the 11th Lunar and Planetary Science Conference, 431–470.

Warren, P.H., (1986). Anorthosite assimilation and the origin of the Mg/Fe-related bimodality of pristine Moon rocks: support for the magmasphere hypothesis. Journal of Geophysical Research, 91, D331–D343.

Warren, P.H. (1993). A concise compilation of petrologic information on possibly pristine nonmare Moon rocks. American Mineralogist, 78, 360–376.

Wieczorek, M.A., et al., (2006). The constitution and structure of the lunar interior. Reviews in Mineralogy and Geochemistry, 60, 221–364.

Wieczorek, M.A., et al., (2013). The crust of the Moon as seen by GRAIL. Science, 339 (6120), 671–675.

Williams, K.B., et al., (2012). The effect of Cr content on the reflectance properties of Mg-spinel. American Geophysical Union, P43A-1905.

Williams, K.B., et al., (in press). Effect of Chromium on Visible-Infrared Spectra of Iron-bearing Aluminate Spinel at Lunar-like Oxygen Fugacity. American Mineralogist, DOI: http://dx.doi.org/10.2138/am-2016-5535

Wood, J.A., et al., (1970). Lunar Anorthosites and a Geophysical Model of the Moon. Proceedings of the Apollo 11 Lunar Science Conference, Vol.1. p. 965-988.

Yamamoto, S., et al., (2013). A new type of pyroclastic deposit on the Moon containing Fe-spinel and chromite. Geophysical Research Letters, 40(1-6).

Zhong, S., Parmentier, E.M., Zuber, M.T., (2000). A dynamic origin for the global asymmetry of lunar mare basalts. Earth and Planetary Science Letters, 177 (3–4), 131–140.

Figure Captions

Figure 1. Natural lunar spinel and olivine in Mg-suite troctolites. Two distinct populations of troctolites exist with respect to spinel composition - pink spinel troctolites (pink filled circles), and chromian-spinel or chromite-bearing troctolites and dunites (blue-green filled circles). **a)** Mg# of olivine vs. the Cr# of spinel and **b)** Mg# of spinel vs. the Cr# of spinel. All data reported are from primary, magmatic spinel within each sample and "Plus signs" indicate PST sample associated with cordierite and chromite-bearing troctolite associated with symplectite assemblages. See Appendix Table 1 for data and references.

Figure 2. Back-scattered electron images of experimental results. **a)** Run A6 (1280^{o}C): Sp = Spinel (Mg# ~91, Cr# ~13) + Ol = olivine (Mg# ~94) + Gl = glass. Tiny Re-metal flakes were observed suspended in the glass phase for this experiment (labeled). Additional small bright spots scattered throughout appear to be spinel nuclei (EDS). **b)** Run D3 (1300^{o}C): Sp (Mg# ~94, Cr# ~5) + Pl = plagioclase + Gl.

Figure 3. Experimental melt compositions (light-blue filled symbols) plotted within Forsterite-Anorthite-Quartz pseudo-ternary space defining experimental phase boundaries (inset highlighted on full ternary and data normalized to wt.% end-member constituents - see *Prissel et al.*, [2014a] for a worked example). Symbol legend provided. 1-atm phase boundaries (dashed gray lines, *Morse* [1980]) relative to estimated phase boundaries from this study (black lines). Modeled melt compositions (open symbols) define ternary peritectic reaction points and spinel-

olivine phase boundaries as a function of initial normative anorthite content (50, 30, and 15% An, labeled within symbols). Cr# of near liquidus spinel also plotted next to each model melt composition (with each model melt composition producing ~Fo95 Olivine, Table 3). Melts undersaturated with plagioclase (15% An) appear to be required for chromite production and several melts with respect to normative anorthite content are required to produce the range of spinel compositions observed in Mg-suite troctolites.

Figure 4. a) Spinel-Olivine $K_D^{Fe\text{-}Mg}$ linearly correlated with the Cr# of spinel. Experimental data (light-blue triangles - this study; open-triangles - *Wan et al.,* [2008], are used to calculate eq. 1 in the text. Natural samples (pink filled circles, PST; blue-green filled circles, troctolites and dunites), and model data (open circles represent near liquidus spinel and olivine compositions and large open circles represent spinel and olivine compositions at plagioclase or orthopyroxene saturation) are plotted relative to the equilibrium trend defined by the experimental data. Symbols are consistent throughout each plot. Sub-solidus re-equilibration will drive the Sp-Ol $K_D^{Fe\text{-}Mg}$ to higher values as FeO diffuses into spinel from olivine (indicated by vertical arrow). PST olivine-spinel pairs are closer to equilibrium compared to those observed within the dunites and troctolites. **b)** Mg# of olivine vs. the Cr# of spinel. Five melt compositions were modeled in the MAGPOX equilibrium crystallization software to test the compositions of Ol + Sp predicted for melts of decreasing %An content in the melt (50 - 15%An in the melt, reported next to each starting composition). **c)** Mg# of spinel vs. the Cr# of spinel. Spinel compositions for the PST, dunites and troctolites have been corrected for sub-solidus re-equilibration (light filled circles are uncorrected).

Figure 5. Mg# of olivine vs. the Mg# of the melt. The olivine-melt $K_D^{Fe\text{-}Mg}$ ~0.30 measured in this study is used to calculate the black curve running through the experimental (light-blue filled squares) and model data (open circles, prior to crystallization Mg# of the melt ~86, ~15% An, Table 3). The range of PST and troctolite (and dunite) olivine compositions is represented by the pink field and blue-green field, respectively. Melts with initially high Mg/Fe and low normative anorthite contents (open circle at melt Mg# ~86) must fractionate appreciable amounts of olivine (> 50%, labeled open circle) to explain olivine compositions in the troctolites and dunites. Thus, a large source of latent heat should be considered in future assimilation and magma-wallrock interaction models.

Figure 1.

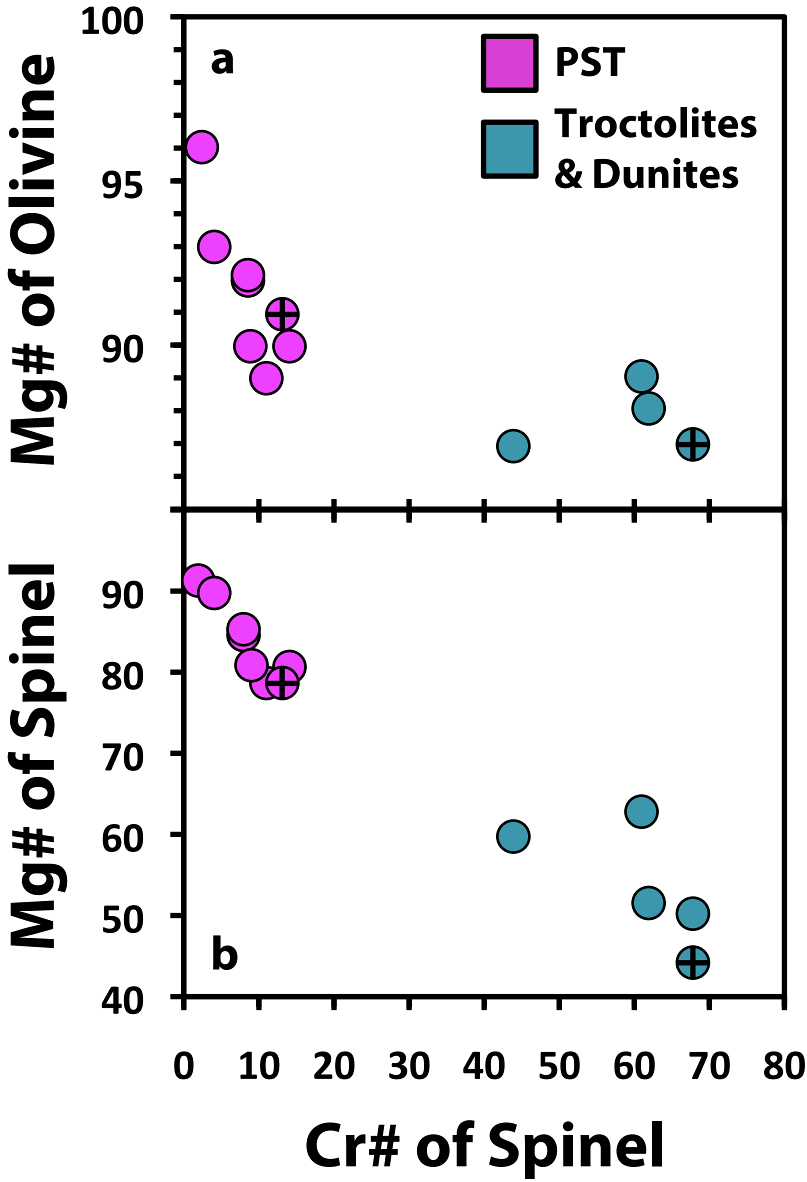

a
b
PST
Troctolites
& Dunites
Mg# of Olivine
Mg# of Spinel
Cr# of Spinel
100
95
90
90
80
70
60
50
40
0
10
20
30
40
50
60
70
80

Figure 2.

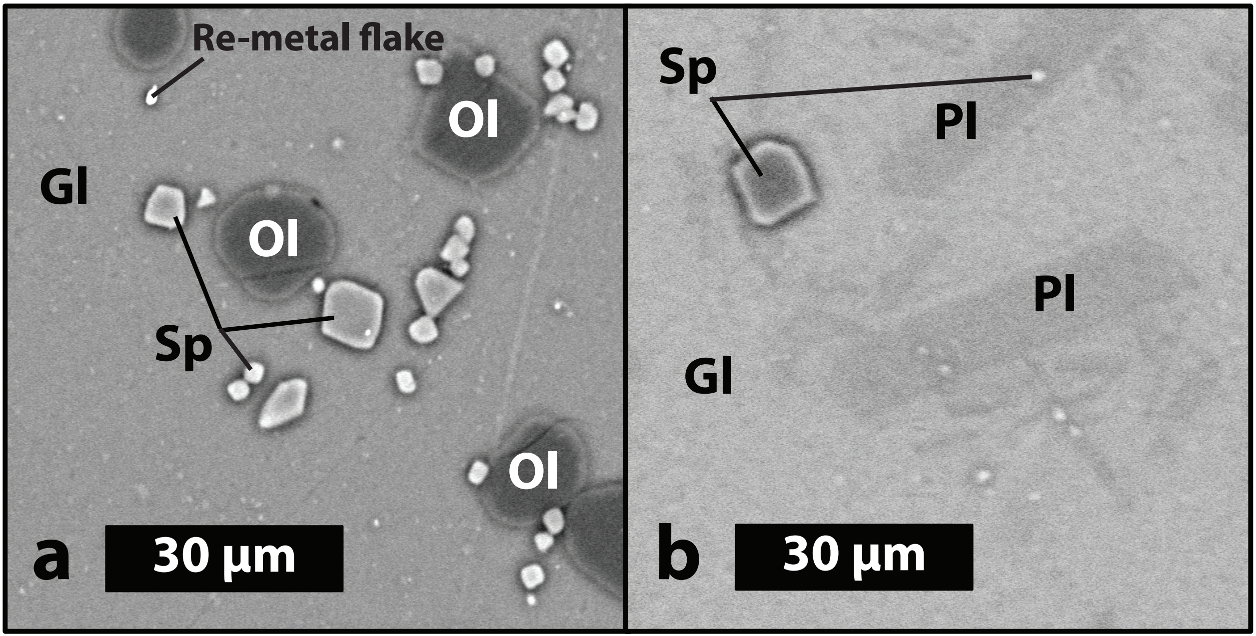

Figure 3.

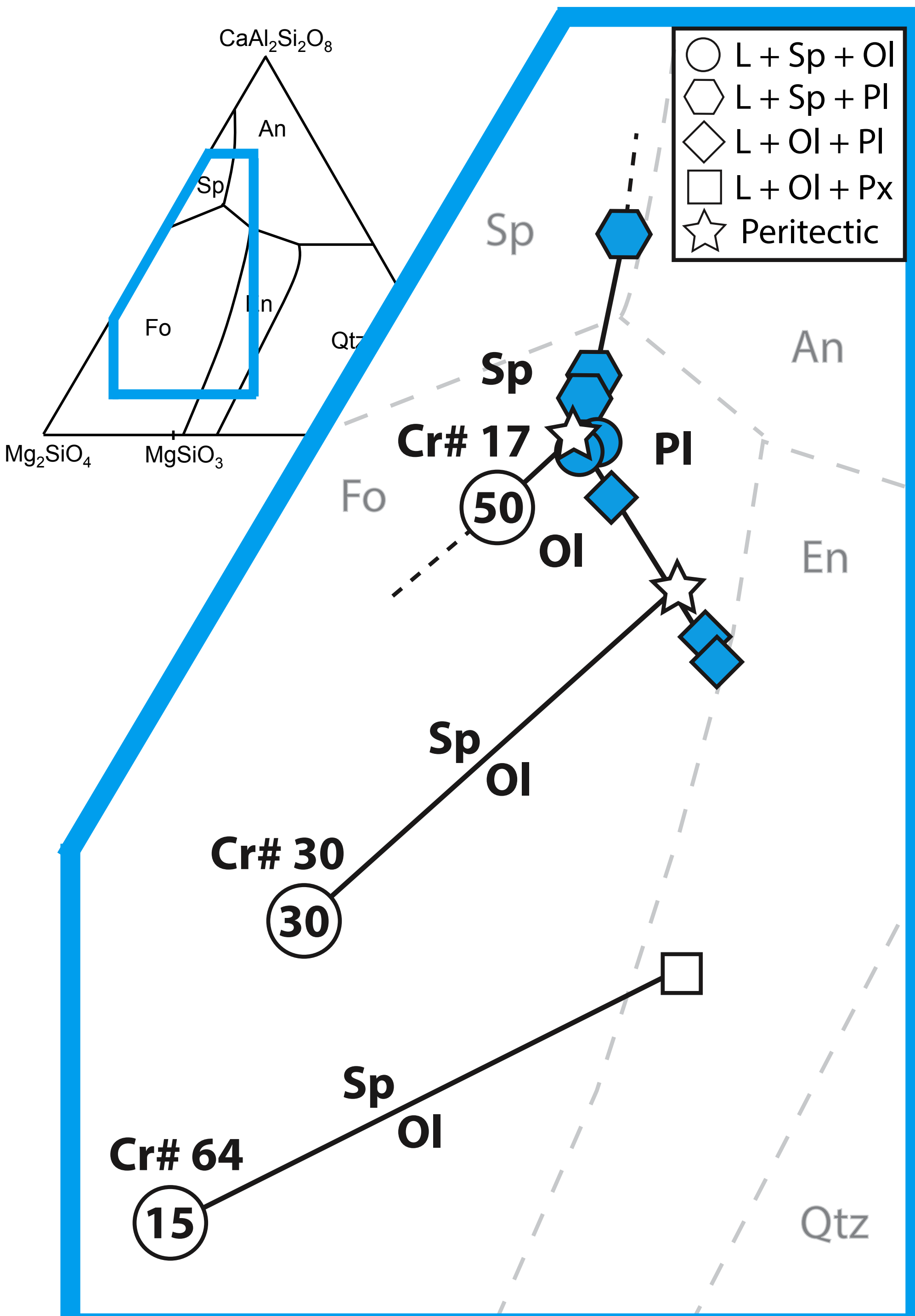

CaAl2Si2O8
An
Sp
Fo
En
Qtz
Mg2SiO4
MgSiO3
L + Sp + Ol
L + Sp + Pl
L + Ol + Pl
L + Ol + Px
Peritectic
Sp
An
Sp
Cr# 17
Pl
Fo
50
Ol
En
Sp
Ol
Cr# 30
30
Sp
Ol
Cr# 64
15
Qtz

Figure 4.

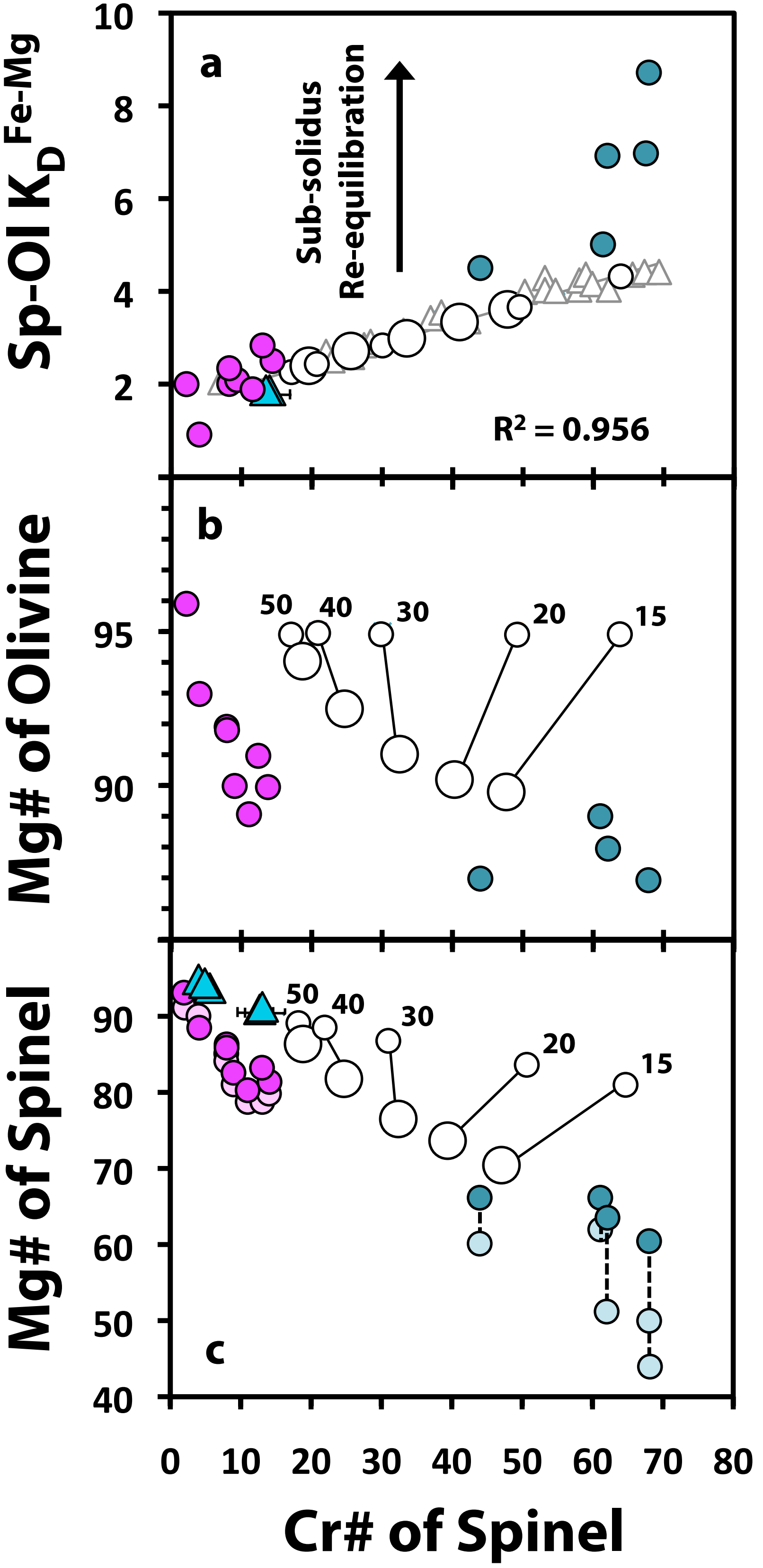

a
b
c
Sub-solidus
Re-equilibration
$R^2 = 0.956$
Sp-Ol $K_D^{Fe\text{-}Mg}$
Mg# of Olivine
Mg# of Spinel
Cr# of Spinel
50
40
30
20
15
0
10
20
30
40
50
60
70
80
2
4
6
8
10
90
95
40
50
60
70
80
90

Figure 5.

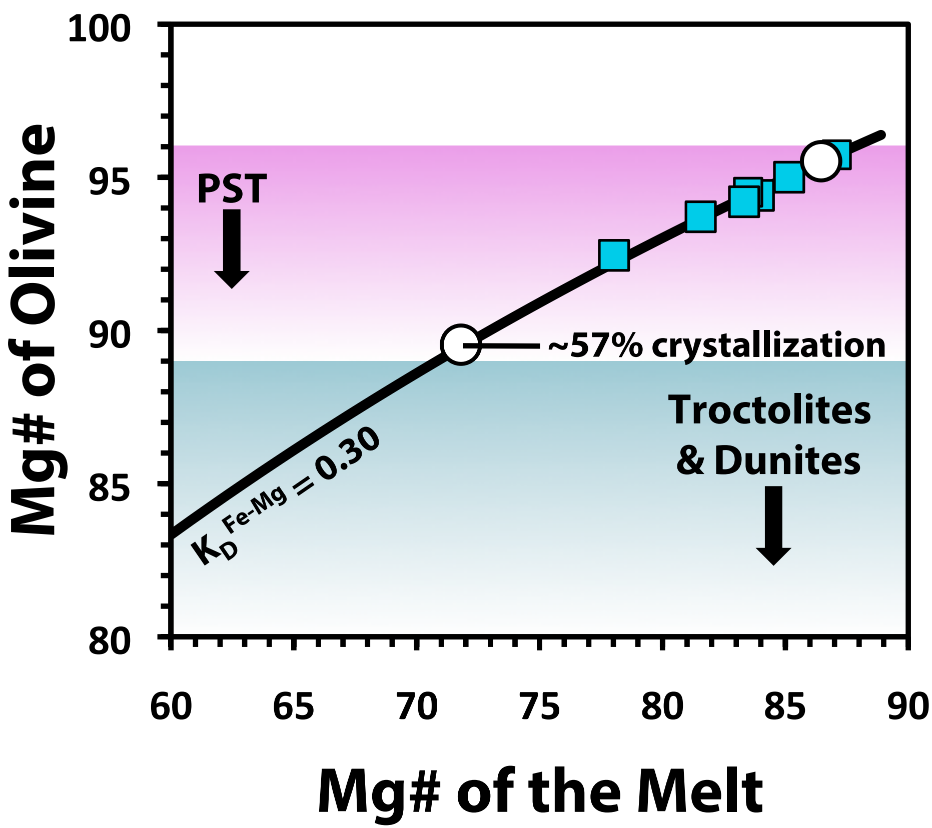

PST
~57% crystallization
Troctolites
& Dunites
$K_D^{Fe\text{-}Mg} = 0.30$
Mg# of Olivine
Mg# of the Melt
100
95
90
85
80
60
65
70
75
80
85
90

Table 1. Experimental starting materials reported in wt.% oxides.

	A		B		C		D	
n	(6)	S.D.	(8)	S.D.	(10)	S.D.	(10)	S.D.
SiO_2	45.8	2	45.8	2	45.1	2	44.4	1
TiO_2	0.93	2	0.75	2	0.65	1	0.47	1
Al_2O_3	17.40	7	21.2	2	22.96	5	26.4	2
Cr_2O_3	0.35	2	0.24	4	0.22	1	0.16	1
FeO[a]	4.8	1	3.8	3	3.5	1	2.6	1
MnO	0.19	4	0.12	6	0.10	5	0.07	3
MgO	17.0	2	13.7	2	12.0	1	8.8	1
CaO	12.45	6	14.12	7	14.92	4	16.4	1
Na_2O	0.19	4	0.14	5	0.16	2	0.19	3
K_2O	0.23	1	0.18	1	0.17	2	0.15	1
Total	**99.4**		**100.0**		**99.8**		**99.6**	
Mg#	86.3	3	86	1	86.0	4	86.0	7
%An	50.2	2	60.0	3	64.9	1	74.1	3

Notes: Glassed compositions were analyzed by EMPA; "n" denotes number of analyses; S.D. denotes 2σ standard deviation on the last significant digit reported; Mg# = cation fraction of [Mg/(Mg + Fe)] x 100; %An = % normative anorthite with respect to Fo-An-Qtz ternary space (see *Prissel et al.,* 2014a for worked example).

[a] FeO = total Iron.

Table 2. Summary of Mg-suite phase equilibria experiments including calculated modal abundance.

Run #	T (^oC)	t (hours)	Gl	S.D.	Ol	S.D.	Pl	S.D.	Sp	S.D.	SSres
A	1400	3	100		-		-		-		-
A3	1330	24	92	3	5	2	-		-		1.51
A4	1300	24	91	2	7	1	-		-		0.58
A6	1280	24	88	1	10	1	-		1.0	7	0.22
A7	1280	24	89.4	8	9.0	6	-		0.8	5	0.09
A5	1225	24	44	5	23	2	30	4	-		0.55
B	1400	3	100		-		-		-		-
B1	1300	24	98	1	-		-		1.8	8	0.36
C	1400	3	100		-		-		-		-
C1	1300	24	84	3	-		13	3	2	1	0.46
D	1400	3	100		-		-		-		-
D2	1350	24	71	4	-		26	4	tr		0.59
D3	1300	24	58	4	-		38	4	tr		0.76
D5	1280	24	35	8	7	3	56	5	-		0.61
D4	1225	24	26	7	10	3	61	5	-		1.20

Notes: All experiments performed at 1-atm pressure and ~IW - 1; Gl = glass, Ol = olivine; Pl = plagioclase, Sp = spinel; SSres denotes the sum of the squared residuals; S.D. denotes 2σ standard deviation on the last significant digit reported; tr = trace amount (mode ~ S.D.).

Table 3. Model Mg-suite parental compositions

	FAN 65315	This Study	Model Input & Results					*Warren* 1986	Komatiite
%An	**-**	**A (50)**	**50**	**40**	**30**	**20**	**15**	**21**	**23**
SiO_2	44.64	45.8	45.8	45.58	45.74	45.90	45.98	46	47.40
TiO_2	0.01	0.93	0.93	1.19	1.39	1.58	1.68	0.3	0.40
Al_2O_3	35.17	17.40	17.40	13.68	10.10	6.49	4.77	7	7.80
Cr_2O_3	0.01	0.35	0.35	0.46	0.53	0.61	0.65	0.5	-
FeO	0.30	4.8	4.8	6.00	6.95	7.91	8.37	12.4	10.8
MnO	0.01	0.19	0.19	0.27	0.31	0.35	0.37	-	-
MgO	0.30	17.0	17.0	21.37	24.88	28.41	30.10	27.6	25.9
CaO	19.25	12.45	12.45	10.42	8.95	7.46	6.76	5.5	7.60
Na_2O	0.30	0.19	0.19	0.44	0.46	0.49	0.50	0.6	0.10
K_2O	0.01	0.23	0.23	0.59	0.69	0.79	0.83	0.06	-
Total	**100**	**99**	**99**	**100**	**100**	**100**	**100**	**100**	**100**
Mg#	-	86	86	86	86	87	87	80	81
Liq T^oC	-	1350 - 1400	1372	1463	1512	1554	1571	1510	1482
Fo#	-	-	95	95	95	95	95	92	93
Cr#	-	-	17	21	30	49	64	46	45
%Xtl	-	10 +/- 1	9.6	29.7	45.3	53.9	57.4	57.9	44.7
Fo#	-	94.3 +/- 0.1	94	93	91	90	90	84	88
Cr#	-	13 +/- 3	19	25	32	40	47	35	35
An#	97	-	98	94	91	OPX	OPX	OPX	OPX

Notes: All iron is assumed to be FeO. Mg# = Mg/(Mg + Fe)x100 of the melt; Liq T = liquidus temperature; Fo# = Mg# of olivine;
Cr# = Cr/(Cr + Al)x100 of spinel; %Xtl = percent crystallized prior to plagioclase or orthopyroxene saturation; An# = Ca/(Ca + Na + K)x100 of plagioclas
OPX denotes orthopyroxene saturation prior to plagioclase saturation. FAN 65315 from *Hess* 1989; komatiite from *Hess* 1994.